
A Review on Heat Transfer Characteristic of Solar Flat Plate Collector

Vibhooti Vaibhav*

Rahul Agarwal**

Jitendra Thakur***

Gaurav Vyas****

Abstract

Nanofluids are engineered colloids, which find a wide range of applications because of their enhanced heat transfer capacity. The nanoparticles, homogeneously dispersed in the base fluid (water in our case) increase the effective thermophysical properties. Nanofluids find a wide range of applications in biomedicines, industries, nuclear reactor cooling, and heat exchangers. In this paper, ceramic nanofluids are used for the enhancement of the heat carrying capacity of base fluid. The thermal behaviour of the nanofluids is derived using the available Nusselt number from the literature. Heat transfer is calculated using practical Nusselt number range. The present work aids in the flow characterization of nanofluids for different geometric specifications of flat plate solar collector and solar ducts.

Keywords:

Nanofluids;
Nusselt Number;
Geometry;
Solar flat plate collector;
Heat transfer characteristic;
Solar radiation.

Author correspondence:

Vibhooti Vaibhav,
Research Scholar, School of Mechanical Engineering
Lovely Professional University, Phagwara, Punjab, India

1. Introduction

The enhancement of heat transfer characteristics of fluids can be characterized by calculating Nusselt number. In this paper, value of Nusselt number is calculated using three different correlations, mentioned in the upcoming sections. The correlations are obtained for flat tube for different geometries, obtained from the literature. The geometries used for the analyses are protrusions for flat tube and solar duct. The range of the parameters is taken from the performed experiments and available work from various authors. The range of operating parameters are set and the change of Nusselt number for distinct parameters is studied. The parameters used in the present work are attack angle, long way length, short way length, Prandtl number, roughness pitch, relative roughness height, relative pipe diameter, volume concentration.

*Research Scholar, School of Mechanical Engineering, Lovely Professional University, Punjab, India

**Research Scholar, School of Mechanical Engineering, Lovely Professional University, Punjab, India

***Research Scholar, School of Mechanical Engineering, Lovely Professional University, Punjab, India

****Assistant Professor, School of Mechanical Engineering, Lovely Professional University, Punjab, India

Authors have reported that the efficiency increases by increasing the glass transmissivity, collector height and particle volume fraction f_v in direct absorption solar collector[1]. Also, the primary sedimentation parameter is flow velocity, which can be controlled by modifying the shape of top and bottom head in solar flat plate collector[2]. Further, the glazing material used has low iron content (<5%) for the reduction of heat infiltration from solar collector to ambient sink[3]. However, density of the nanofluid is proportional to the volume fraction of the nanoparticles [4], which increases the required pumping power for the flow of fluids. Furthermore, the performance of a solar collector is influenced by orientation and tilt angle with the horizontal as the reference plane [5]. Also, use of nanofluid improves the thermal conductivity of the fluid. Studies suggest the enhancement of thermal conductivity due to dispersion of nanoparticles, increment of turbulence, Brownian motion and thermophoresis[6].

2. Research Methodology

Table 1. Nusselt Number correlation used for the analyses

Geometry	Correlation
Protrusions[7]	$Nu = 0.154 \times Re^{1.017} \times \left(\frac{P}{e}\right)^{-0.38} \times \left(\frac{e}{D}\right)^{0.521} \times \left(\frac{\alpha}{60}\right)^{-0.213} \times \exp\left[-2.023 \left(\ln\left(\frac{\alpha}{60}\right)\right)^2\right]$ <p style="text-align: right;">(1)</p>
Flat tube[8]	$Nu = 0.023 Re^{0.8} Pr^{0.3} \left(1 + 0.1771 \phi^{0.1465}\right)$ <p style="text-align: right;">(2)</p>
Protrusions[9]	$Nu = 2.1 \times 10^{-88} Re^{1.452} (S/e)^{12.94} (L/e)^{99.2} (d/D)^{-3.9} \times \exp\left[(-10.4)\{\log(S/e)\}^2\right]$ $\times \exp\left[(-77.2)\{\log(L/e)\}^2\right]$ $\times \exp\left[(-7.83)\{\log(d/D)\}^2\right]$ <p style="text-align: right;">(3)</p>

3. Results and Analysis

3.1 Model 1

Figure 1 displays the change in Nusselt range for variation in Reynolds range for distinctive values of frictional pitch. As the cost of Reynolds quantity growth, it's miles determined that the cost of Nusselt quantity also increases. The graph is plotted for special values of relative roughness pitch. The variety of relative roughness pitch is between 12 to 24. The graph shows a linear relation among Reynolds wide variety and Nusselt wide variety for the particular range used inside the correlation.

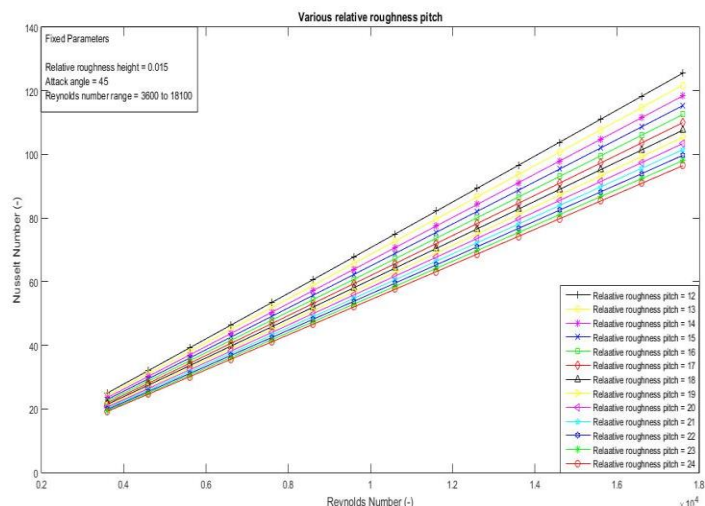


Figure 1. Change of Nusselt number with respect to Reynolds number for variation in roughness characteristics

Figure 2 demonstrates the connection among Nusselt number and Reynolds number for varying estimations of roughness characteristics. Observed behaviour for Nusselt number increments with increment for Reynolds number in specific scope of the relationship being utilized. The estimation of Nusselt number additionally increment with increment in relative roughness height. This proposes Nusselt number and relative roughness height are straightforwardly related for this specific correlation.

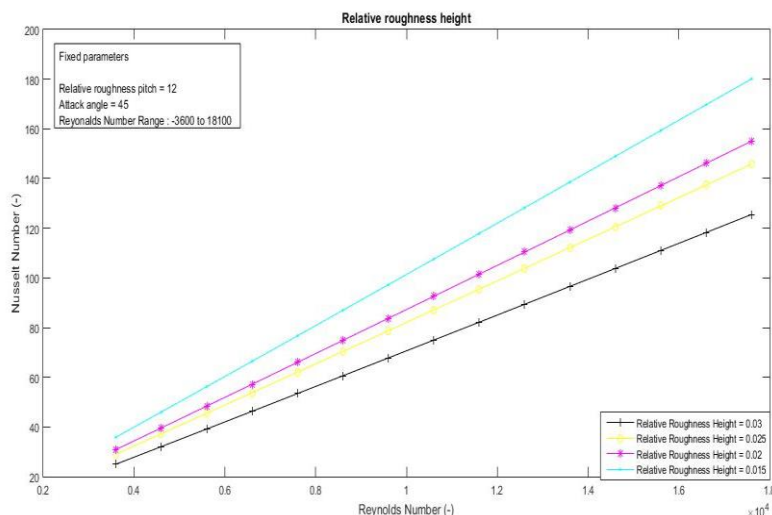


Figure 2. Alteration of Nusselt number with respect to Reynolds number for different values of relative roughness height

Figure 3 depicts that Nusselt range and Reynolds wide variety are directly proportional. Nusselt quantity will increase with a growth in the value of Reynolds number. The graph is plotted for distinct values of attack angle. The range of Nusselt number increases with growth within the attack angle up to a value after which starts falling down. The present computational work shows range for Nusselt number increment from 45 degrees to 60 ranges and then starts falling down as much as seventy-five degrees.

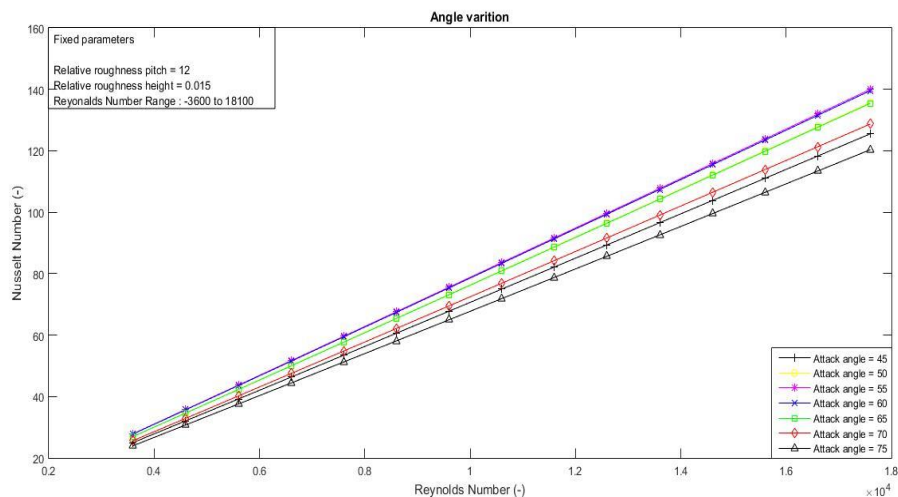


Figure 3. Alteration of Nusselt number with respect to Reynolds number for distinct attack angle

Model - 2

Figure 4 reflects the version of Nusselt number with distinct Reynolds number for a number 3000 to 8000. It replicates the range of Nusselt number increment with rise in Reynolds number. The particle volume concentration is changed and graph among Reynolds range and Nusselt number varies. The range of particle volume concentration is zero to 0.06. We have a look at that the range of Nusselt number increasing with boom within the volume concentration of nanoparticle.

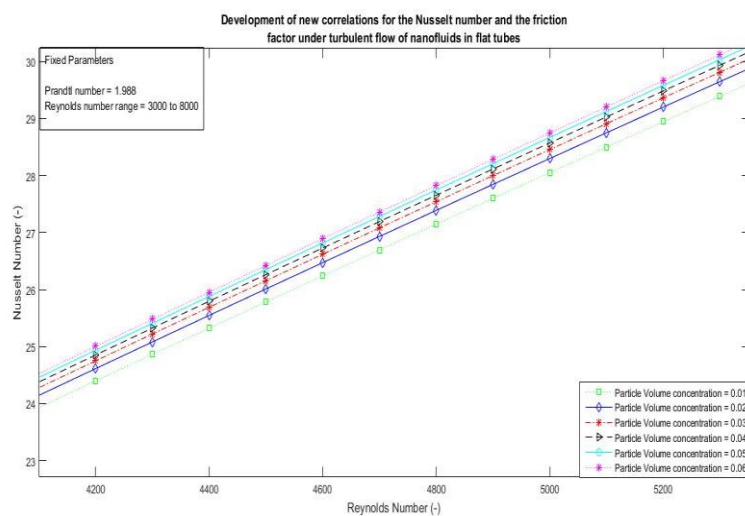


Figure 4. Alteration of Nusselt number for Reynolds number with distinct particle volume concentration

Figure 5 reflects the alteration of the Nusselt number with variation in Reynolds number range. The graph proves the records that Reynolds number and Nusselt number are without delay proportional and that they boom together. The graph is plotted for various values of Prandtl

number. The range of Prandtl number for the correlation is between 1.988 to 13.44. With variation in Prandtl number the Nusselt number has extended.

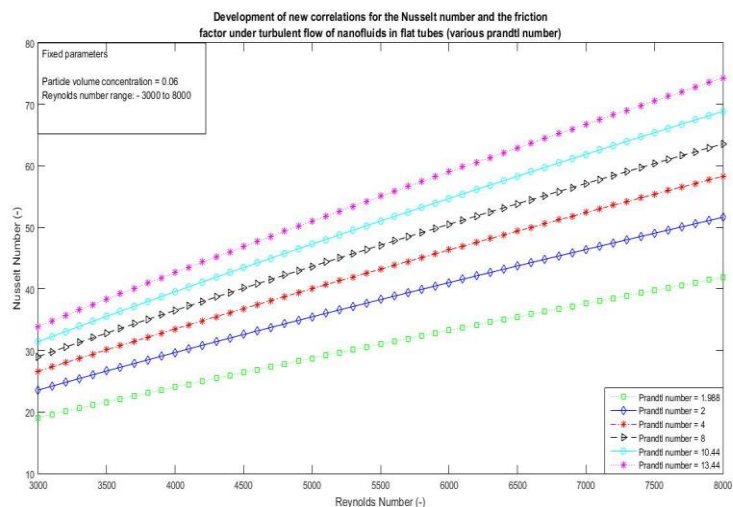


Figure 5. Alteration of Nusselt number with respect to Reynolds number for various distinct values of Prandtl number

Model-3

Figure 6 suggests the variation of Nusselt number range with admire to Reynolds number. Obtained value of Nusselt number will increase of Reynolds number. The above graph is plotted for various values of relative long way length whose duration is among 25 to 37.50. Value of Nusselt number changes with relative long length way period and then begins falling.

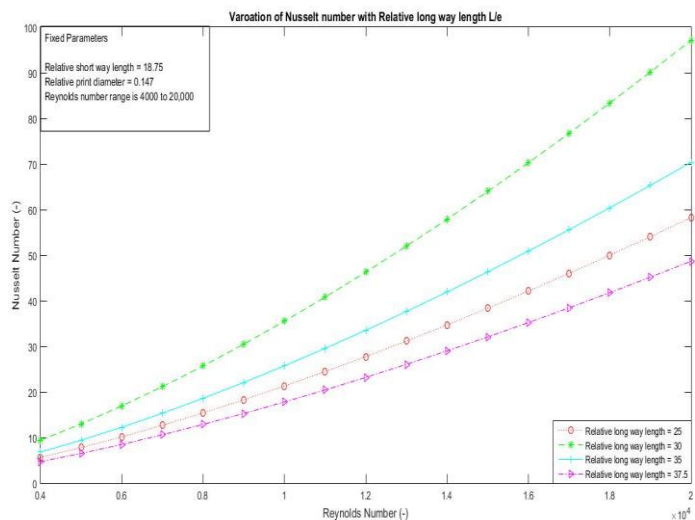


Figure 6. Variation of Nusselt number with respect to Reynolds number for various relative long way length

Figure 7 shows the variation of Nusselt wide variety with Reynolds number range. Nusselt number seems to increase with growth in Reynolds number. The above graph is plotted for specific values of short way length. The range of Nusselt number will increase with growth in relative short way length up to a sure limit and starts falling for increased value of relative short way length.

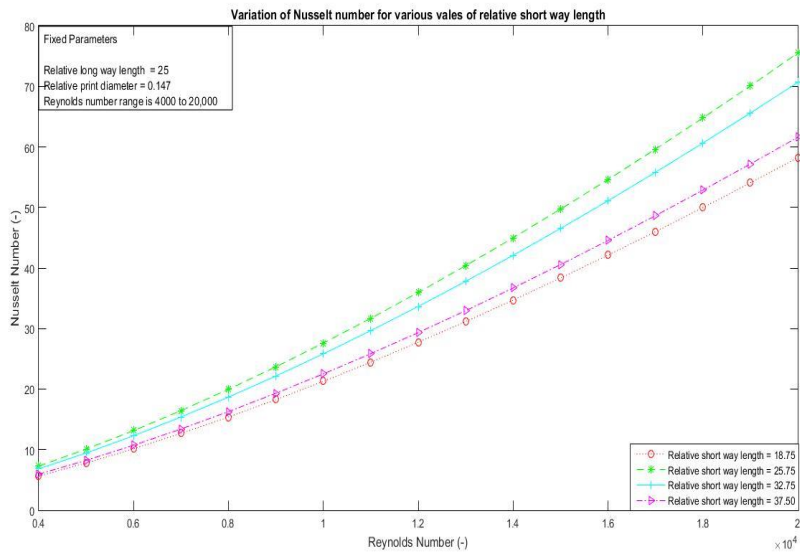


Figure 7. Alteration of Nusselt number with respect to Reynolds number for various distinct value of short way length

Figure 8 indicates the version of Nusselt number with respect to Reynolds number. Observed variation of Nusselt number increments with boom inside Reynolds number range. Nusselt number is calculated for specific values of relative print diameter. Observed the range of Nusselt number will increment as much as certain restrict with the print diameter but begins reducing after that value.

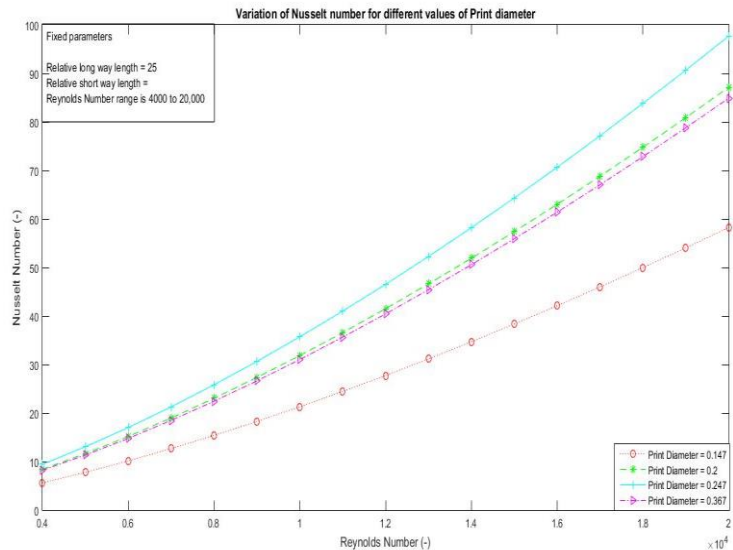


Figure 8. Alteration of Nusselt number with Reynolds number for various distinct value of print diameter

4. Conclusion

Relation between Nusselt number and Reynolds number plotted for three distinct correlations. Various parameters have been incorporated in the correlation and the range of the parameters is kept specific for different configurations. It is observed that the increase in Reynolds range, increases the Nusselt number, thereby increasing the thermal performance of the system. Increasing the volume concentration also results in an increase of Nusselt number. In model one, the value of Nusselt number is seen to grow with frictional characteristics within the specified range. But after a certain roughness value, Nusselt number starts decreasing. In case of flat tube, Nusselt number elevates with increased volume concentration and Prandtl number. Nusselt number also elevates up to a certain limit of long way length and relative short way length. Nusselt number was also observed to decrease after a certain value of relative pipe diameter.

References

- [1] H. Tyagi, P. Phelan, and R. Prasher, "Predicted Efficiency of a Low-Temperature Nanofluid-Based Direct Absorption Solar Collector," *J. Sol. Energy Eng.*, vol. 131, no. 4, p. 41004, 2009.
- [2] G. Colangelo, E. Favale, A. De Risi, and D. Laforgia, "A new solution for reduced sedimentation flat panel solar thermal collector using nanofluids," *Appl. Energy*, vol. 111, pp. 80–93, 2013.
- [3] A. Alvarez, O. Cabeza, M. C. Muñiz, and L. M. Varela, "Experimental and numerical investigation of a flat-plate solar collector," *Energy*, vol. 35, no. 9, pp. 3707–3716, 2010.
- [4] M. Faizal, R. Saidur, S. Mekhilef, and M. A. Alim, "Energy, economic and environmental analysis of metal oxides nanofluid for flat-plate solar collector," *Energy Convers. Manag.*, vol. 76, pp. 162–168, 2013.
- [5] H. Gunerhan and A. Hepbasli, "Determination of the optimum tilt angle of solar collectors for building applications," *Build. Environ.*, vol. 42, no. 2, pp. 779–783, 2007.
- [6] H. K. Gupta, G. Das Agrawal, and J. Mathur, "Investigations for effect of Al₂O₃-H₂O nanofluid flow rate on the efficiency of direct absorption solar collector," *Case Stud. Therm. Eng.*, vol. 5, pp. 70–78, 2015.
- [7] S. Yadav, M. Kaushal, Varun, and Siddhartha, "Nusselt number and friction factor correlations for solar air heater duct having protrusions as roughness elements on absorber plate," *Exp. Therm. Fluid Sci.*, vol. 44, pp. 34–41, 2013.
- [8] R. S. Vajjha, D. K. Das, and D. R. Ray, "International Journal of Heat and Mass Transfer Development of new correlations for the Nusselt number and the friction factor under turbulent flow of nanofluids in flat tubes," *HEAT MASS Transf.*, vol. 80, pp. 353–367, 2015.
- [9] B. Bhushan and R. Singh, "Nusselt number and friction factor correlations for solar air heater duct having artificially roughened absorber plate," *Sol. Energy*, vol. 85, no. 5, pp. 1109–1118, 2011.